Recovery of 3-D Motion and Structure from Image Correspondences Using a Directional Confidence Measure

Gilad Adiv
Edward Riseman

COINS TR 88-105

December 1988

RECOVERY OF 3-D MOTION AND STRUCTURE FROM IMAGE CORRESPONDENCES USING A DIRECTIONAL CONFIDENCE MEASURE

*Gilad Adiv**
Edward Riseman

ABSTRACT

We present a new scheme for computing 3-D motion and structure from a flow field representing either image velocities or image displacements between two frames. This scheme is based on a global least-squares technique, introduced in [Adi85a,b], for minimizing the deviation between the given flow field and the field predicted by the hypothesized 3-D motion and structure. Here, this technique is generalized by assigning a *directional confidence measure* to each flow vector. This confidence measure is defined by two orthogonal axes and corresponding confidence values, representing the reliability of the estimated image motion along each axis. It is shown how to relate these confidence values to the error distributions of the estimated flow values. The directional confidence measure is especially useful for recovering 3-D information from correspondences of line segments or edge points, where the normal component of the image motion is much more reliable than the tangential component. Experiments based on simulated and real data demonstrate the improvement achieved by employing a directional confidence measure instead of a scalar confidence measure. Finally, we show that the reliability of depth estimates can be predicted from the confidence measure.

---

* The author is with Rafael, POB 2250(34), Haifa 31021, Israel. Most of this work was performed when he was a visiting scientist at the Computer and Information Science Department, University of Massachusetts, Amherst, MA 01003.

1. INTRODUCTION

The problem of passive navigation, where a sensor is moving through a stationary environment, is one of the major research issues in the area of dynamic visual interpretation. Given two perspective views from such a sensor, it is possible to extract the 3-D motion of the sensor and the structure of the environment, up to a scaling factor. Such information can be used to control the motion of vehicles or robots.

The most common approach for the analysis of visual motion is based on two phases. The first phase is computation of image correspondences, usually referred to as an optical flow field, or a displacement field. The second phase consists of an interpretation of this field. Many of the algorithms described in the literature use point correspondences in the second phase (e.g., [Ull79], [Lon81], [Bru81], [Tsa84], [Adi85a,b]). Given an image point, we know that it is the projection of one of an infinite number of points in the 3-D space, all of them located on a ray defined by the image point and the lens center. The correspondence of a point in the first image to a point in the second image means that the two 3-D rays associated with these points intersect each other. This puts a constraint on the problem and, therefore, given a sufficient number of point correspondences, the 3-D motion and structure can be extracted (up to a scaling factor).

Recently, a few authors have proposed to compute 3-D motion and structure from line correspondences (e.g., [Liu88], [Fau87], [Spe87]), utilizing the information given by the orientation and the distance from the origin of the lines. This new approach may be very useful in man-made environments where straight lines are dominant and stable features. It has been found, however, that correspondence of a line in two frames does not sufficiently constrain the problem; that is, the 3-D motion and structure can not be

recovered from such information. To understand this, notice that a line in the image is associated with a plane in the 3-D space containing all the 3-D lines possibly generating the image line. A correspondence of a line in the first image to a line in the second image is equivalent, therefore, to the intersection of the two associated 3-D planes. Unfortunately, two arbitrary planes generally intersect each other and, therefore, no constraint on the motion parameters can be obtained from such an intersection. Thus, line correspondences over three frames are necessary for recovery of 3-D motion.

In all interesting applications measurements of image motion are corrupted by noise. Therefore, the recovery of 3-D motion and structure should be based on the minimization of some error function of these 3-D variables. Such a function is usually the sum of error terms, where each term is associated with one image correspondence. The contribution of this term to the global error function should depend on the reliability of the related image motion measurement. In [Bru81] and [Adi85a,b] the overall reliability of each flow vector is assumed to be estimated and represented by a *scalar confidence measure*. This measure was integrated into a least-squares scheme for minimizing the sum of deviations between the measured flow vectors and the corresponding vectors predicted by the hypothesized 3-D parameters.

Anandan [Ana87, Ana88] has introduced a more general confidence measure, which we call the *directional confidence measure*. This measure can be employed as a tool for improving the representation of knowledge about uncertainties of image motion measurements. It is defined by two orthogonal axes and corresponding confidence values, giving the reliability of the estimation of displacement along each axis. Typically, the axis with maximal confidence value will be oriented in the direction of the image gradient. Anandan has applied such a directional confidence measure to the estimation of a dense displace-

ment field. In this technique, each displacement vector is assigned a directional confidence measure, based on the curvatures of an error surface associated with the measurements for determining this vector. The confidence measure is employed to control the smoothing between adjacent vectors. A similar "oriented smoothness" approach is taken by Nagel and Enkelmann [Nag86], but without recognizing the implicit use of a directional confidence measure.

We will employ the directional confidence measure as a tool for developing a unified approach for solving 3-D motion and structure from point and line correspondences. This tool is especially important in the case of line correspondences, and we will use this case for motivating our approach. We have already concluded that line correspondences over three frames are apparently necessary for recovering 3-D motion. Using a third frame is roughly equivalent to using second-order time derivatives of the line parameters. However, such derivatives can not be expected to be recovered reliably in the presence of noise, and this solution may be particularly sensitive to noise if the three viewpoints are close to each other.

In this paper we present another approach. Usually, endpoints of lines in the image can be extracted, and the lines are given as line *segments*. We argue that, utilizing the information given by the location of line endpoints, the 3-D motion and structure can be estimated reliably using only *two* frames. In other words, we will introduce a method for recovering 3-D interpretation consistent not only with the line equations, but also with the location of the endpoints along the line (Fig. 1). This approach can also be regarded as a specific case of solving motion and structure from point correspondences.

Of course, the determination of an endpoint location along a line may be a difficult

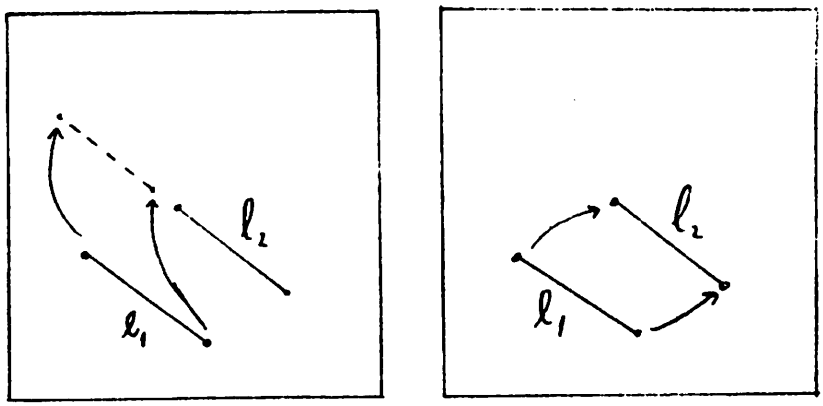

Fig. 1: Correspondence of lines with and without endpoint correspondence. l_1 is a line segment in the first frame and l_2 is a corresponding line segment in the second frame. (a) A 3-D solution that transforms l_1 as shown is supported by this 2-D line correspondence if consistency of the line equations is the only criterion. It is not supported if, in addition, an overlapping of the line segments is required. (b) In this more restrictive sense, a 3-D solution that transforms the endpoints of l_1 to the endpoints of l_2 is maximally supported by the line correspondence.

task, and sensitive to noise. On the other hand, the transverse location of the endpoint can be expected to be measured accurately. Therefore, when evaluating the consistency of a hypothesized 3-D solution with image correspondences of line segments, the deviation along a line should be allowed to be larger than the deviation in the transverse direction (see Fig. 2).

This observation can be given a mathematical formulation by giving the longitudinal deviation a relatively small weight, while giving the transverse deviation a relatively large weight. In other words, the directional confidence measure is suitable for representing our knowledge about the uncertainty of an endpoint location. This approach was already demonstrated by Wells [Wel87] in a constrained case, where the motion is known and the goal is to recover the location of 3-D line segments projected on a sequence of images.

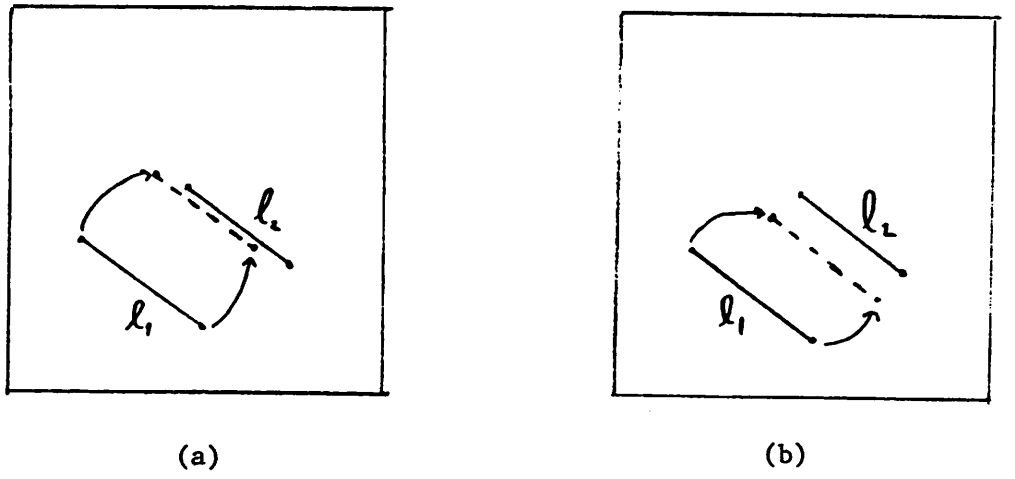

(a) (b)

Fig. 2: Uncertainty in line segment position. The uncertainty of the line segment position in the longitudinal direction is much larger than the uncertainty in the transverse direction. (a) Correspondence of line segments l_1 and l_2 is consistent with this uncertainty and, therefore, it supports the realted 3-D transformation. (b) Correspondence is inconsistent with uncertainty in line segment position. Thus, it does not support the realted 3-D transformation.

In the following sections we will develop a general scheme for using a directional confidence measure. As has already been noted, such a scheme is especially needed in the case of line segment correspondences, but it may also improve the results in other cases when 3-D information must be extracted from feature correspondences or optical flow. Given, for example, corner correspondences, one may want to give a higher confidence to the direction perpendicular to the bisector of the angle of an acute corner. Finally, notice that this scheme is relevant not only to motion analysis, but also to stereoscopic vision and image matching.

2. A MATHEMATICAL FORMULATION

2.1 Relating Image Motion to 3-D Motion and Structure

In this section we show how the motion of image features is related to the 3-D camera motion and the 3-D environmental structure, assuming a perspective projection. The camera motion is allowed to be general, with six degrees of freedom, but the environment is assumed to be stationary in this treatment.

Let (X,Y,Z) represent a cartesian coordinate system which is fixed with respect to the camera (see Fig. 3), and let (x,y) represent a corresponding coordinate system of a planar image. The focal length, from the nodal point O to the image, is assumed to be known. It can be normalized to 1 without loss of generality. Thus, the perspective projection (x,y) on the image of a point (X,Y,Z) in the environment is:

$$x = X/Z, \qquad y = Y/Z. \tag{1}$$

The motion of the camera between two time instances, t and t', can be decomposed into two components: rotation $\underline{\Omega} = (\Omega_X, \Omega_Y, \Omega_Z)$ about an axis through the origin, followed by translation $\underline{T} = (T_X, T_Y, T_Z)$. If (X,Y,Z) and (X',Y',Z') are the coordinates at times t and t', respectively, of a point in the environment, then

$$\begin{pmatrix} X' \\ Y' \\ Z' \end{pmatrix} = R \begin{pmatrix} X \\ Y \\ Z \end{pmatrix} - \underline{T}, \tag{2a}$$

where the rotation matrix R can be approximated, assuming small values of the rotation

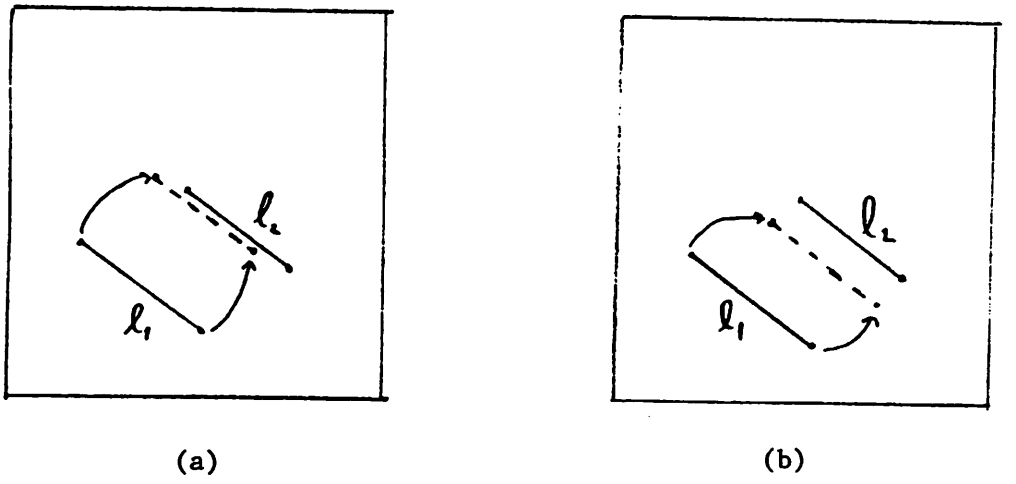

Fig. 2: Uncertainty in line segment position. The uncertainty of the line segment position in the longitudinal direction is much larger than the uncertainty in the transverse direction. (a) Correspondence of line segments l_1 and l_2 is consistent with this uncertainty and, therefore, it supports the realted 3-D transformation. (b) Correspondence is inconsistent with uncertainty in line segment position. Thus, it does not support the realted 3-D transformation.

In the following sections we will develop a general scheme for using a directional confidence measure. As has already been noted, such a scheme is especially needed in the case of line segment correspondences, but it may also improve the results in other cases when 3-D information must be extracted from feature correspondences or optical flow. Given, for example, corner correspondences, one may want to give a higher confidence to the direction perpendicular to the bisector of the angle of an acute corner. Finally, notice that this scheme is relevant not only to motion analysis, but also to stereoscopic vision and image matching.

2. A MATHEMATICAL FORMULATION

2.1 Relating Image Motion to 3-D Motion and Structure

In this section we show how the motion of image features is related to the 3-D camera motion and the 3-D environmental structure, assuming a perspective projection. The camera motion is allowed to be general, with six degrees of freedom, but the environment is assumed to be stationary in this treatment.

Let (X, Y, Z) represent a cartesian coordinate system which is fixed with respect to the camera (see Fig. 3), and let (x, y) represent a corresponding coordinate system of a planar image. The focal length, from the nodal point O to the image, is assumed to be known. It can be normalized to 1 without loss of generality. Thus, the perspective projection (x, y) on the image of a point (X, Y, Z) in the environment is:

$$x = X/Z, \qquad y = Y/Z. \tag{1}$$

The motion of the camera between two time instances, t and t', can be decomposed into two components: rotation $\underline{\Omega} = (\Omega_X, \Omega_Y, \Omega_Z)$ about an axis through the origin, followed by translation $\underline{T} = (T_X, T_Y, T_Z)$. If (X, Y, Z) and (X', Y', Z') are the coordinates at times t and t', respectively, of a point in the environment, then

$$\begin{pmatrix} X' \\ Y' \\ Z' \end{pmatrix} = R \begin{pmatrix} X \\ Y \\ Z \end{pmatrix} - \underline{T}, \tag{2a}$$

where the rotation matrix R can be approximated, assuming small values of the rotation

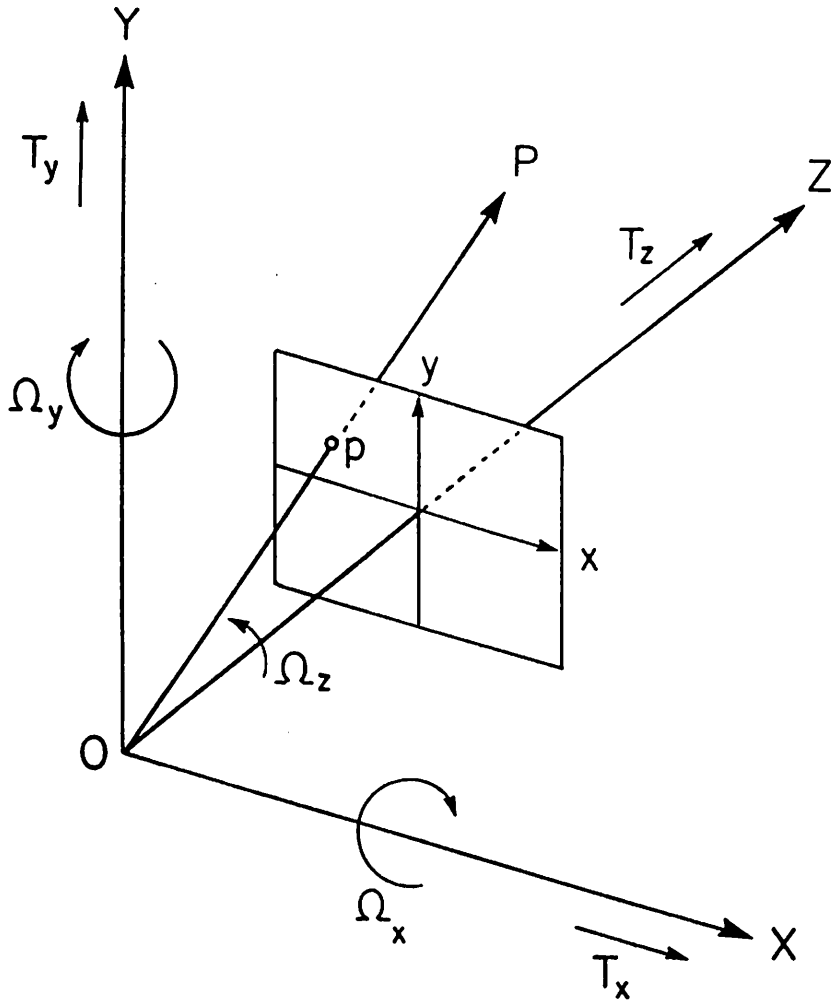

Fig. 3: Coordinate systems. A coordinate system (X, Y, Z) attached to the camera, and the corresponding image coordinates (x, y). The image position $\underline{p}$ is the perspective projection of the point $\underline{P}$ in the environment. $\underline{T} = (T_X, T_Y, T_Z)$ and $\underline{\Omega} = (\Omega_X, \Omega_Y, \Omega_Z)$ represent the translation and rotation of the camera.

parameters, by

$$R = \begin{pmatrix} 1 & \Omega_Z & -\Omega_Y \\ -\Omega_Z & 1 & \Omega_X \\ \Omega_Y & -\Omega_X & 1 \end{pmatrix}. \tag{2b}$$

Now, let (x, y) and (x', y') be the image points corresponding to (X, Y, Z) and

(X', Y', Z'), respectively, and let (α, β) be the displacement vector $(x' - x,\ y' - y)$. Then, from Eqs. (1) and (2) we get:

$$\alpha = X'/Z' - X/Z = \frac{1}{Z}\Big(x'Z - X\Big) =$$

$$= \frac{1}{Z}\Big[x'(Z' - \Omega_Y X + \Omega_X Y + T_Z) - (X' - \Omega_Z Y + \Omega_Y Z + T_X)\Big] =$$

$$= \Omega_X x'y - \Omega_Y(1 + xx') + \Omega_Z y + (-T_X + T_Z x')/Z. \tag{3a}$$

Similarly, we can obtain:

$$\beta = \Omega_X(1 + yy') - \Omega_Y xy' - \Omega_Z x + (-T_Y + T_Z y')/Z. \tag{3b}$$

These equations were previously introduced by Medioni and Yasumoto [Med85]. Notice that

$$\begin{pmatrix} \alpha \\ \beta \end{pmatrix} = \begin{pmatrix} \alpha_R \\ \beta_R \end{pmatrix} + \begin{pmatrix} \alpha_T \\ \beta_T \end{pmatrix}, \tag{4a}$$

where (α_R, β_R) and (α_T, β_T) are, respectively, the rotational and translational components of the displacement field:

$$\begin{pmatrix} \alpha_R \\ \beta_R \end{pmatrix} = \begin{pmatrix} x'y \\ 1 + yy' \end{pmatrix} \Omega_X + \begin{pmatrix} -1 - xx' \\ -xy' \end{pmatrix} \Omega_Y + \begin{pmatrix} y \\ -x \end{pmatrix} \Omega_Z, \tag{4b}$$

$$\begin{pmatrix} \alpha_T \\ \beta_T \end{pmatrix} = \begin{pmatrix} -T_X/Z \\ -T_Y/Z \end{pmatrix} + \begin{pmatrix} x' \\ y' \end{pmatrix} T_Z/Z. \tag{4c}$$

As can easily be verified, if x' and y' are replaced by x and y, respectively, then Eqs. (4) express the relations between image *velocities* (α, β) and spatial *velocities*

$(\Omega_X, \Omega_Y, \Omega_Z)$ and (T_X, T_Y, T_Z). In this case, the assumption of small rotation parameters is no longer needed. In the rest of this paper, the term 'flow' refers to both 'displacement' and 'velocity'.

Our basic goal is to extract the motion parameters $\underline{T}$, $\underline{\Omega}$ and the depth values $\{Z\}$ from the flow vectors $\{(\alpha, \beta)\}$, using the relations (4). It is easy to see, however, that $\underline{T}$ and $\{Z\}$ can only be determined up to a scaling factor. Therefore, we will introduce new parameters which represent the extractable information.

Let r be the magnitude of the translation. Assuming that r is non-zero, we define new parameters which are possible to estimate:

$$\underline{U} = \underline{T}/r \tag{5}$$

and

$$\tilde{Z} = r/Z. \tag{6}$$

$\underline{U} = (U_X, U_Y, U_Z)$ is a unit vector, representing the direction of the 3-D translation, and $\tilde{Z}$ represents a normalized version of the reciprocal depth, which we find more convenient to estimate and analyze than Z/r. Employing these normalized parameters, Eq. (4a) can be rewritten as

$$\begin{pmatrix} \alpha \\ \beta \end{pmatrix} = \begin{pmatrix} \alpha_R \\ \beta_R \end{pmatrix} + \begin{pmatrix} \alpha_U \\ \beta_U \end{pmatrix} \tilde{Z}, \tag{7}$$

where

$$\begin{pmatrix} \alpha_U \\ \beta_U \end{pmatrix} = \begin{pmatrix} \alpha_T \\ \beta_T \end{pmatrix} / \tilde{Z} = - \begin{pmatrix} U_X \\ U_Y \end{pmatrix} + \begin{pmatrix} x' \\ y' \end{pmatrix} U_Z. \tag{8}$$

2.2 Scalar and Directional Confidence Measures

Let us assume that each flow vector is assigned a confidence measure. In the past we used a measure represented by a scalar, W, giving the overall reliability of the flow estimate [Ana84], [Adi85a,b]. A more general approach is to use a directional quantity, represented by two orthogonal axes and corresponding confidence measures. Along one axis the confidence, denoted by W_t, is maximal, while along the other axis the confidence, denoted by W_l, is minimal. The angle between the axis of maximal confidence and the x-axis is given by ρ ($0 \leq \rho < 180°$). Geometrically, the scalar measure can be represented by a circle with radius W, while the directional measure can be represented by an ellipse with a long axis W_t and a short axis W_l (see Fig. 4).

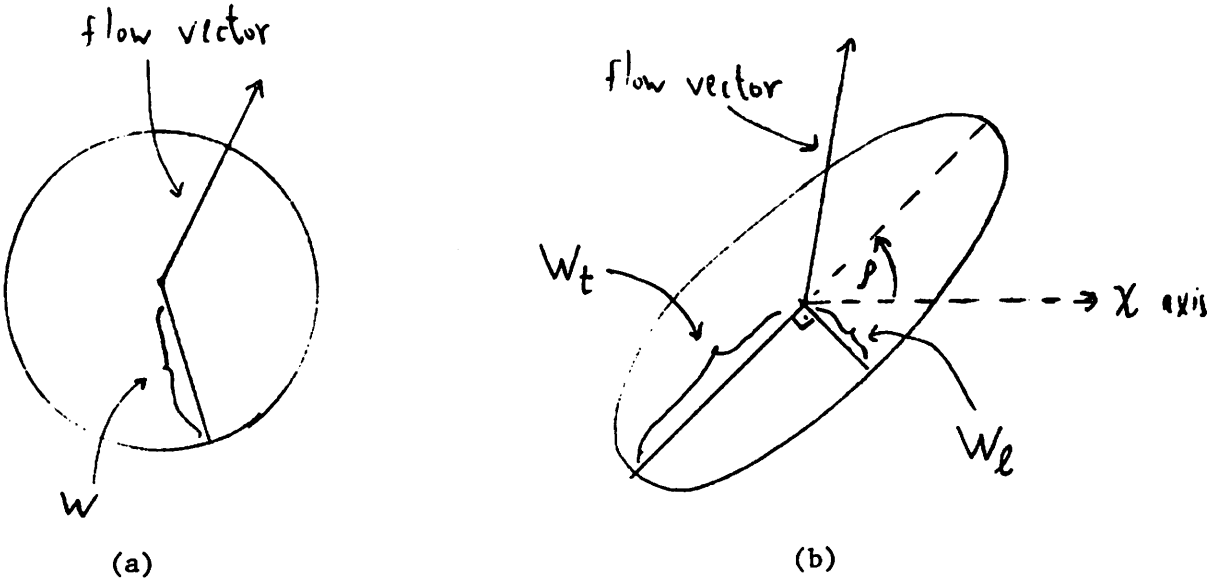

Fig. 4: Geometrical interpretation of scalar and directional confidence measures. (a) The circle represents a scalar confidence measure, where the confidence is uniform with respect to the direction. ((b) The ellipse represents a directional confidence measure, where the confidence varies as a function of the direction.

A directonal confidence measure is computed in [Ana87, Ana88] for a dense displacement field. Typically, in uniform regions both minimal and maximal confidence values are low, whereas at edges (except occlusion boundaries) the confidence is high along the gradient direction and low along the edge, and finally at corners both values are high.

The confidence measure (either scalar or directional) can be used for weighting the contribution of the flow vector to the determination of 3-D motion and structure parameters. In order to save computation, it is also possible to select and use a given number of "best" flow vectors, while ignoring the other vectors.

3. A GLOBAL OPTIMIZATION APPROACH USING A SCALAR CONFIDENCE MEASURE

Before turning to the directional confidence measure, we show in this section how knowledge, represented by a *scalar* confidence measure, can be integrated into a least squares scheme for extracting 3-D motion and structure from optical flow. Let $(\alpha_1,\beta_1),\ldots,(\alpha_n,\beta_n)$ be n flow vectors measured at the image points $(x_1,y_1),\ldots,(x_n,y_n)$ and assigned scalar confidence values $W_1,\ldots,W_n$. The goal is to extract 3-D motion parameters, $\underline{U}$ and $\underline{\Omega}$, and normalized depth values, $\tilde{Z}_1,\ldots,\tilde{Z}_n$, which are maximally consistent with the available data.

Let us briefly review the approach in [Bru81] and [Adi85a,b], where a least squares scheme is employed. This approach, which is attractive because of its relative robustness to noise, is based on minimizing the deviation between the measured flow vectors and those predicted from the estimated 3-D motion parameters and depth values. The deviation related to each flow vector is weighted by the corresponding confidence value. In other

words, we want to find $\underline{U}$, $\underline{\Omega}$ and $\tilde{Z}_1,\ldots,\tilde{Z}_n$ such that the error function

$$\sum_{i=1}^{n} W_i[(\alpha_i - \alpha_{Ri} - \alpha_{Ui}\tilde{Z}_i)^2 + (\beta_i - \beta_{Ri} - \beta_{Ui}\tilde{Z}_i)^2] \tag{9}$$

is minimized (see Eq. (7)). In addition, the constraints $\tilde{Z}_i \geq 0$, $i = 1,\ldots,n$, should be satisfied, but, for the sake of brevity, we ignore them in the current discussion. The interested reader is referred to [Adi85a,b].

Given the values of the motion parameters, the optimal value of $\tilde{Z}_i$, $1 \leq i \leq n$, can be found by minimizing the corresponding term in the error function (9):

$$\tilde{Z}_i = \frac{(\alpha_i - \alpha_{Ri})\alpha_{Ui} + (\beta_i - \beta_{Ri})\beta_{Ui}}{\alpha_{Ui}^2 + \beta_{Ui}^2}. \tag{10}$$

Substituting (10), for any $1 \leq i \leq n$, into (9) and expanding the resulting expression yields the following representation of the error, as a function of the motion parameters:

$$E(\underline{U},\underline{\Omega}) = \sum_{i=1}^{n} W_i \frac{[(\alpha_i - \alpha_{Ri})\beta_{Ui} - (\beta_i - \beta_{Ri})\alpha_{Ui}]^2}{\alpha_{Ui}^2 + \beta_{Ui}^2}. \tag{11}$$

The motion parameters are recovered in [Adi85a,b] by deriving from (11) an error measure which correpsponds to possible values of $\underline{U}$. For each hypothesized $\underline{U}$, the optimal rotation parameters and a related error value are computed by solving three linear equations. A minimum value of the resulting error function is determined, using a multi-resolution sampling technique.

A directonal confidence measure is computed in [Ana87, Ana88] for a dense displacement field. Typically, in uniform regions both minimal and maximal confidence values are low, whereas at edges (except occlusion boundaries) the confidence is high along the gradient direction and low along the edge, and finally at corners both values are high.

The confidence measure (either scalar or directional) can be used for weighting the contribution of the flow vector to the determination of 3-D motion and structure parameters. In order to save computation, it is also possible to select and use a given number of "best" flow vectors, while ignoring the other vectors.

3. A GLOBAL OPTIMIZATION APPROACH USING A SCALAR CONFIDENCE MEASURE

Before turning to the directional confidence measure, we show in this section how knowledge, represented by a *scalar* confidence measure, can be integrated into a least squares scheme for extracting 3-D motion and structure from optical flow. Let $(\alpha_1,\beta_1),\ldots,(\alpha_n,\beta_n)$ be n flow vectors measured at the image points $(x_1,y_1),\ldots,(x_n,y_n)$ and assigned scalar confidence values $W_1,\ldots,W_n$. The goal is to extract 3-D motion parameters, $\underline{U}$ and $\underline{\Omega}$, and normalized depth values, $\tilde{Z}_1,\ldots,\tilde{Z}_n$, which are maximally consistent with the available data.

Let us briefly review the approach in [Bru81] and [Adi85a,b], where a least squares scheme is employed. This approach, which is attractive because of its relative robustness to noise, is based on minimizing the deviation between the measured flow vectors and those predicted from the estimated 3-D motion parameters and depth values. The deviation related to each flow vector is weighted by the corresponding confidence value. In other

words, we want to find $\underline{U}$, $\underline{\Omega}$ and $\tilde{Z}_1,\ldots,\tilde{Z}_n$ such that the error function

$$\sum_{i=1}^{n} W_i[(\alpha_i - \alpha_{Ri} - \alpha_{Ui}\tilde{Z}_i)^2 + (\beta_i - \beta_{Ri} - \beta_{Ui}\tilde{Z}_i)^2] \tag{9}$$

is minimized (see Eq. (7)). In addition, the constraints $\tilde{Z}_i \geq 0$, $i = 1,\ldots,n$, should be satisfied, but, for the sake of brevity, we ignore them in the current discussion. The interested reader is referred to [Adi85a,b].

Given the values of the motion parameters, the optimal value of $\tilde{Z}_i$, $1 \leq i \leq n$, can be found by minimizing the corresponding term in the error function (9):

$$\tilde{Z}_i = \frac{(\alpha_i - \alpha_{Ri})\alpha_{Ui} + (\beta_i - \beta_{Ri})\beta_{Ui}}{\alpha_{Ui}^2 + \beta_{Ui}^2}. \tag{10}$$

Substituting (10), for any $1 \leq i \leq n$, into (9) and expanding the resulting expression yields the following representation of the error, as a function of the motion parameters:

$$E(\underline{U},\underline{\Omega}) = \sum_{i=1}^{n} W_i \frac{[(\alpha_i - \alpha_{Ri})\beta_{Ui} - (\beta_i - \beta_{Ri})\alpha_{Ui}]^2}{\alpha_{Ui}^2 + \beta_{Ui}^2}. \tag{11}$$

The motion parameters are recovered in [Adi85a,b] by deriving from (11) an error measure which correpsponds to possible values of $\underline{U}$. For each hypothesized $\underline{U}$, the optimal rotation parameters and a related error value are computed by solving three linear equations. A minimum value of the resulting error function is determined, using a multi-resolution sampling technique.

4. A GLOBAL OPTIMIZATION APPROACH USING A DIRECTIONAL CONFIDENCE MEASURE

4.1 Error Functions and a Search Procedure

In this section we generalize the analysis of the previous section by assuming that a *directional* confidence measure is assigned to each flow vector. Let (W_{ti}, W_{li}, ρ_i) represent the directional confidence corresponding to the measured flow vector (α_i, β_i), $1 \leq i \leq n$ (see Section 2.2). In order to weight correctly the deviation between the measured and predicted flow vectors, a rotated coordinate system is separately determined for each vector, using ρ_i as the angle of rotation. Values in a rotated coordinate system will be denoted by the symbol ' ', e.g. (see Fig. 5):

$$\begin{pmatrix} \alpha_i' \\ \beta_i' \end{pmatrix} = \begin{pmatrix} \cos\rho_i & \sin\rho_i \\ -\sin\rho_i & \cos\rho_i \end{pmatrix} \begin{pmatrix} \alpha_i \\ \beta_i \end{pmatrix}. \tag{12}$$

Following Eq. (9), the error function to be minimized is

$$\sum_{i=1}^{n} [W_{ti}(\alpha_i' - \alpha_{Ri}' - \alpha_{Ui}'\tilde{Z}_i)^2 + W_{li}(\beta_i' - \beta_{Ri}' - \beta_{Ui}'\tilde{Z}_i)^2] \tag{13}$$

Again, we can find the optimal value of $\tilde{Z}_i$, as a function of the motion parameters, by minimizing the corresponding term in the error function. This can be done by examining the first derivative of (13), with respect to $\tilde{Z}_i$, and setting it equal to 0. Thus, we get

$$\tilde{Z}_i = \frac{W_{ti}(\alpha_i' - \alpha_{Ri}')\alpha_{Ui}' + W_{li}(\beta_i' - \beta_{Ri}')\beta_{Ui}'}{W_{ti}\alpha_{Ui}'^2 + W_{li}\beta_{Ui}'^2}. \tag{14}$$

Substituting (14), for any $1 \leq i \leq n$, into (13) and expanding the resulting expression

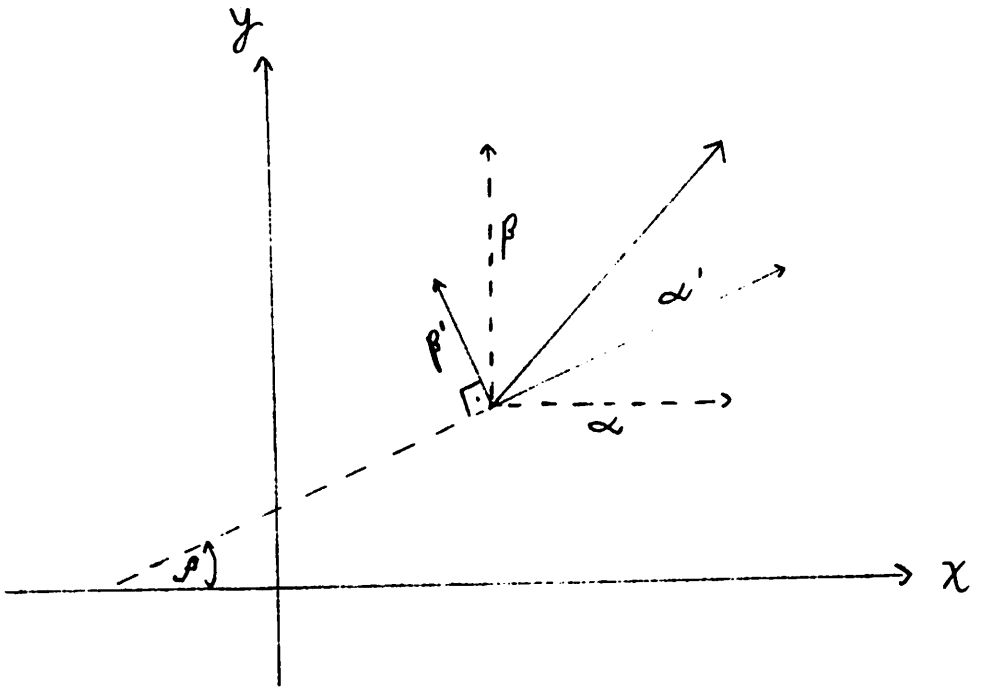

Fig. 5: Rotating a coordinate system via the confidence vector. The flow vector (α,β) is given in the image coordinate system (x,y). The angle ρ corresponds to the axis with maximal confidence. It defines a rotated coordinate system in which α' and β' are the new flow values.

yields the following representation of the error, as a function of the motion parameters:

$$E(\underline{U},\underline{\Omega}) = \sum_{i=1}^{n} \frac{W_{ti}W_{li}[(\alpha'_i - \alpha'_{Ri})\beta'_{Ui} - (\beta'_i - \beta'_{Ri})\alpha'_{Ui}]^2}{W_{ti}{\alpha'_{Ui}}^2 + W_{li}{\beta'_{Ui}}^2}. \tag{15}$$

The search for optimal $\underline{U}$ and $\underline{\Omega}$ can be based on the search procedure outlined in the previous section. The values of α'_i and β'_i, $1 \leq i \leq n$, can be determined by applying Eq. (12). Similarly, the coefficients of the rotation parameters in α'_{Ri} and β'_{Ri}, $1 \leq i \leq n$, can be determined from the corresponding coefficients in α_{Ri} and β_{Ri} (see Eq. (4b)). For a given $\underline{U}$, the values of α'_{Ui} and β'_{Ui}, $1 \leq i \leq n$, can be computed from α_{Ui} and β_{Ui} (see Eq. (8)). Thus, for each hypothesized value of $\underline{U}$, the problem becomes a least squares

problem with expressions which *linearly* depend on Ω_X, Ω_Y and Ω_Z. These rotation parameters and a corresponding error measure can, therefore, be computed by solving three linear equations. Thus, an error function, defined on the unit sphere, is obtained. As in Section 3, this function can be minimized using a multi-resolution sampling technique.

4.2 Discussion

A few interesting observations can easily be made from Eqs. (14) and (15):

1) Given a flow vector (α, β) for which $W_l \ll W_t$ (e.g., a point along an edge but not at a corner), one can estimate the corresponding depth by

$$\tilde{Z} \approx \frac{\alpha' - \alpha'_R}{\alpha'_U}, \tag{16}$$

unless ${\alpha'_U}^2 \ll {\beta'_U}^2$. This estimate is only based on the one reliable component of the flow vector. If, for example, we deal with a line correspondence, then the transverse component of the line displacement will be the dominant one in determining the depth, unless this component is much smaller than the longitudinal component of the displacement.

2) If $W_l = 0$, then, according to Eq. (15), the corresponding flow vector gives no constraint on the optimal motion parameters. This is consistent with the observation already made in the literature that line correspondences in two frames do not constrain the problem. However, assuming that the motion parameters are known (e.g., via the constraints from the other flow vectors in the optimization process), the corresponding depth value (see (16)) may still be recovered.

3) Assuming that $0 < W_l \ll W_t$, the related error measure is

$$e \approx \frac{W_l}{{\alpha'_U}^2}[(\alpha' - \alpha'_R)\beta'_U - (\beta' - \beta'_R)\alpha'_U]^2. \tag{17}$$

Thus, the contribution e of a flow vector to the total error measure is principally determined by the value of W_l. However, even if W_l is small, e may be large if $|\alpha'_U| \ll |\beta'_U|$. Given a line correspondence, for example, this means that the hypothesized focus of expansion (FOE) is along the line. In this case, we have

$$e \approx W_l\left(\frac{\beta'_U}{\alpha'_U}\right)^2(\alpha' - \alpha'_R)^2. \tag{18}$$

Therefore, in order to minimize e, α'_R should be close to α'. In the case of a line correspondence, the transverse component of the motion predicted by the hypothesized rotation should be similar to the transverse component of the measured displacement.

Suppose now that line correspondences are determined and an FOE is hypothesized such that there exist lines approximately oriented towards it. Applying the previous discussion, we can check whether there exist rotation parameters consistent with the transverse displacements of these lines and, thus, either compute the rotation parameters or refute the hypothesis. For example, it is possible to compute the rotation parameters of a sensor moving along a road by using the boundary lines of the road.

5. RELATING CONFIDENCE MEASURES TO NOISE DISTRIBUTIONS

In this section we show how confidence values can be derived from probabilistic estimates of measurement errors of flow vectors. Suppose that each flow vector is corrupted by an additive noise with two orthogonal components, N_t and N_l. It is assumed that the expectations of N_t and N_l are 0 and that their standard deviations, σ_t and σ_l, satisfy $0 < \sigma_t \leq \sigma_l$. The angle, denoted by ρ, between the axis corresponding to N_t and the x-axis may be different for each flow vector ($0° \leq \rho < 180°$). Following the analysis and notations in Section 4.1, a coordinate system rotated by ρ_i, $1 \leq i \leq n$, is introduced for each flow vector (α_i, β_i), and the corresponding values are denoted by the symbol ''.

Employing the least squares scheme, it is desirable to normalize each deviation by the expected value of the related measurement error. Hence, the error function to be minimized should be

$$\sum_{i=1}^{n}\left[\left(\frac{\alpha_i' - \alpha_{Ri}' - \alpha_{Ui}'\tilde{Z}_i}{\sigma_{ti}}\right)^2 + \left(\frac{\beta_i' - \beta_{Ri}' - \beta_{Ui}'\tilde{Z}_i}{\sigma_{li}}\right)^2\right]. \tag{19}$$

Thus, each deviation is measured in units of the standard deviation of the related measurement error, and the penalty for the deviation is determined by this normalized value. Notice that Eq. (19) leads us to Eq. (13) with

$$W_{ti} = 1/\sigma_{ti}^2 , \qquad W_{li} = 1/\sigma_{li}^2 . \tag{20}$$

In the framework of the least squares technique with a scalar confidence measure, the deviations are computed in the x and y axes. Let N_x and N_y be the corresponding

measurement errors. Their standard deviations, σ_x and σ_y, satisfy the equalities

$$\sigma_x^2 + \sigma_y^2 = \mu(N_x^2 + N_y^2) = \mu(N_t^2 + N_l^2) = \sigma_t^2 + \sigma_l^2, \tag{21}$$

where μ denotes expectation, in a probabilistic sense. In addition, N_x and N_y are equally distributed and, therefore,

$$\sigma_x^2 = \sigma_y^2 = (\sigma_t^2 + \sigma_l^2)/2 \; . \tag{22}$$

For estimating the 3-D motion and structure, we should minimize the expression

$$\sum_{i=1}^{n} \Big[\Big(\frac{\alpha_i - \alpha_{Ri} - \alpha_{Ui}\tilde{Z}_i}{\sigma_x} \Big)^2 + \Big(\frac{\beta_i - \beta_{Ri} - \beta_{Ui}\tilde{Z}_i}{\sigma_y} \Big)^2 \Big]. \tag{23}$$

Using Eq. (22), this leads us to Eq. (9) with

$$W_i = 2/(\sigma_{ti}^2 + \sigma_{li}^2). \tag{24}$$

The definitions (20) and (24) of W_t, W_l and W yield the following relation between the directional and scalar confidence measures:

$$W = \frac{2}{\sigma_t^2 + \sigma_l^2} = \frac{2}{1/W_t + 1/W_l} = \frac{2W_tW_l}{W_t + W_l} \; . \tag{25}$$

This relation will be employed in Experiment 2 for obtaining a scalar confidence measure out of the given directional confidence measure.

6. A CONFIDENCE MEASURE FOR DEPTH ESTIMATES

Many experimental results show that depth estimates are often inaccurate (see, for example, the careful study in [Dut88]). This problem is inherent near the FOE or when

the translation is small relative to the distance of the camera from the observed surface [Adi89]. It is important, therefore, to define a confidence measure for the depth estimates, thus making it possible to distinguish between reliable and unreliable results.

As in the previous section, let us again assume that the flow field is corrupted by an additive noise (N_t, N_l). In addition to the properties and definitions already stated in Section 5, we assume that N_t and N_l are uncorrelated. Using the directional confidence measure, the depth estimate is given by Eq. (14). Assuming that the motion parameters are accurately recovered, the variance of each depth estimate is

$$\sigma^2(\tilde{Z}) = \frac{W_t^2\,\sigma_t^2\,{\alpha'_U}^2 + W_l^2\,\sigma_l^2\,{\beta'_U}^2}{\left(W_t{\alpha'_U}^2 + W_l{\beta'_U}^2\right)^2}. \tag{26}$$

Substituting W_t and W_l with $1/\sigma_t^2$ and $1/\sigma_l^2$, as proposed in the previous section, we obtain:

$$\sigma^2(\tilde{Z}) = \frac{1}{\left(\alpha'_U/\sigma_t\right)^2 + \left(\beta'_U/\sigma_l\right)^2} \tag{27}$$

We can now define a confidence measure for $\tilde{Z}$:

$$C(\tilde{Z}) \stackrel{\text{def}}{=} 1/\sigma^2(\tilde{Z}) = W_t\,{\alpha'_U}^2 + W_l\,{\beta'_U}^2. \tag{28}$$

Notice that this confidence measure is small near the FOE, where α'_U and β'_U are close to 0.

Eventually, we are usually interested in estimating Z/r, that is, $1/\tilde{Z}$. Denoting Z/r by Z^*, we can obtain the following equalities, where estimated values are denoted by small letters:

$$\Delta Z^* \stackrel{\text{def}}{=} z^* - Z^* = 1/\tilde{z} - 1/\tilde{Z} = \frac{\tilde{Z} - \tilde{z}}{\tilde{Z}\tilde{z}} = \frac{-\Delta\tilde{Z}}{\tilde{Z}\tilde{z}}. \tag{29}$$

Thus, the relative error in the estimated depth is

$$|\Delta Z'|/Z' = |\Delta \tilde{Z}|/\tilde{z} \approx |\Delta \tilde{Z}|/\tilde{Z} = |\Delta \tilde{Z}|\frac{Z}{r}, \tag{30}$$

where the approximation above is justified if the relative error in estimating $\tilde{Z}$ is small. In this case,

$$\sigma^2(\Delta Z^*/Z^*) \approx \frac{Z^2/r^2}{(\alpha'_U/\sigma_t)^2 + (\beta'_U/\sigma_l)^2} = \frac{1}{(\alpha'_T/\sigma_t)^2 + (\beta'_T/\sigma_l)^2}, \tag{31}$$

and a confidence measure can be defined as

$$C(\Delta Z^*/Z^*) = \frac{r^2}{Z^2}(W_t {\alpha'_U}^2 + W_l {\beta'_U}^2) = W_t {\alpha'_T}^2 + W_l {\beta'_T}^2. \tag{32}$$

As a conclusion, the estimated value of Z/r becomes more reliable as the ratio between the translation magnitude and Z is increased. In addition, notice that the reliability is determined by the ratios, σ_t/α'_T and σ_l/β'_T, between the expected measurement errors and the corresponding translational components. A reliable depth estimate can be expected only if at least one of these ratios is small.

7. EXPERIMENTS

In this section we compare results achieved by employing either a scalar confidence measure or a directional confidence measure. The first experiment is based on simulated data, while the other two are based on images taken from a video camera translating through a hallway in the direction of the line of sight.

7.1 Experiment 1

The first experiment simulates a camera translating along the line of sight at speed

of one (focal) unit per second. This motion can be represented by $\underline{T} = (0., 0., 1.)$ and $\underline{\Omega} = (0.°, 0.°, 0.°)$. The environment consists of two planar surfaces parallel to the image plane. A background plane is in a distance of 20 units from the image plane. It is occluded around its intersection with the line of sight by the second surface, which is a planar patch in a distance of 10 units from the image plane. The field of view of the camera is $30°$, and the image contains 512×512 pixels.

Velocity vectors are uniformly sampled in the image. Each vector is perturbed by additive noise, with two orthogonal and independent components, N_t and N_l. These noise components are assumed to be uniformly distributed in the intervals $[-0.5, 0.5]$ and $[-6., 6.]$, respectively, where values are given in units of pixels per second. The angle ρ, between the x-axis and the axis corresponding to N_t, is uniformly distributed in the interval $[0.°, 180.°)$.

The motion and depth values were computed from the flow data using both the scheme with scalar confidence measure and the scheme with directional confidence measure. In the first case, the confidence values should be identical for each velocity vector. In the second case, following the discussion in Section 5, $W_t/W_l = (6/0.5)^2 = 144$.

A statistical study of the results was performed, based on 200 experiments with each of the schemes. In 100 experiments 64 velocity vectors were used, while in the other experiments 256 vectors were used. In each experiment the noise values were randomly sampled. The results, shown in Table 1, demonstrate the significant improvement achieved by using the directional confidence measure. Relative to the scheme based on scalar confidence measure, there is an improvement of more than 50% in estimating the motion parameters, and more than 60% in estimating the normalized depth values. Notice that

a similar improvement in the estimation of the motion parameters (but not in the depth values) has been achieved by using 256 flow vectors instead of 64 vectors.

Errors	# Vectors	Scalar Confidence	Directional Confidence
ΔU	64	2.20°	1.05°
	256	0.88°	0.32°
$\|\Omega\|$	64	0.158°	0.078°
	256	0.078°	0.030°
$\|\Delta\tilde{Z}\|/\tilde{Z}$	64	23.4%	9.5%
	256	18.7%	6.3%

Table 1: Experiment 1. The average errors in the direction of the translation vector and in the magnitude of rotation, and the average relative error in the depth values.

7.2 Experiment 2

This experiment is based on a dense displacement field and a related directional confidence measure computed by Anandan's technique [Ana88]. The experiment demonstrates the ability to recover 3-D motion and structure from such estimates of image motion, using either a scalar confidence measure or a directional confidence measure. The input images (of 256×256 pixels), the displacement field and the maximal component of the directional confidence measure are shown in Fig. 6, Fig. 7 and Fig. 8, respectively. The field of view of the camera is 25°.

The confidence values, computed by Anandan's technique, can take any non-negative number. We assumed, however, that the standard deviation of the least accurate displacement measurements is at most 10 times the standard deviation of the most accurate measurements. Therefore, we transformed the confidence values W into the interval

(a)

(b)

Fig. 6: Experiment 2: the intensity images.

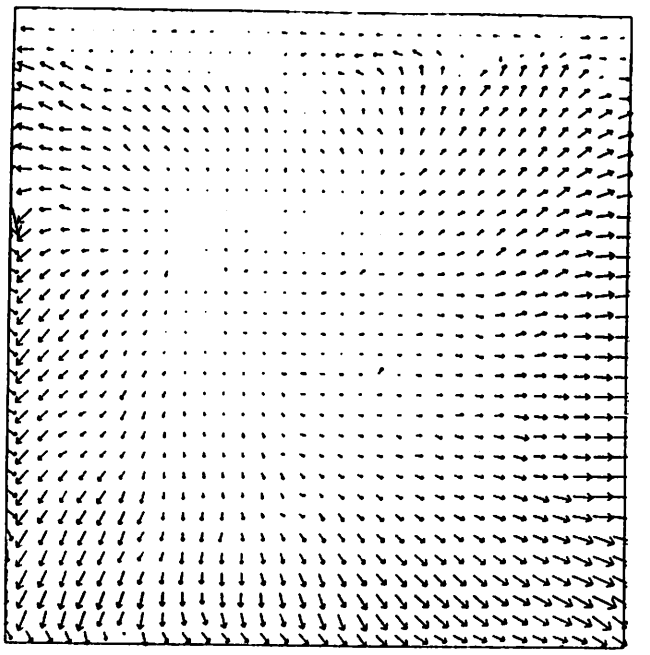

Fig. 7: Experiment 2: a 32×32 sample of the computed flow field. The vectors are scaled by 1.2.

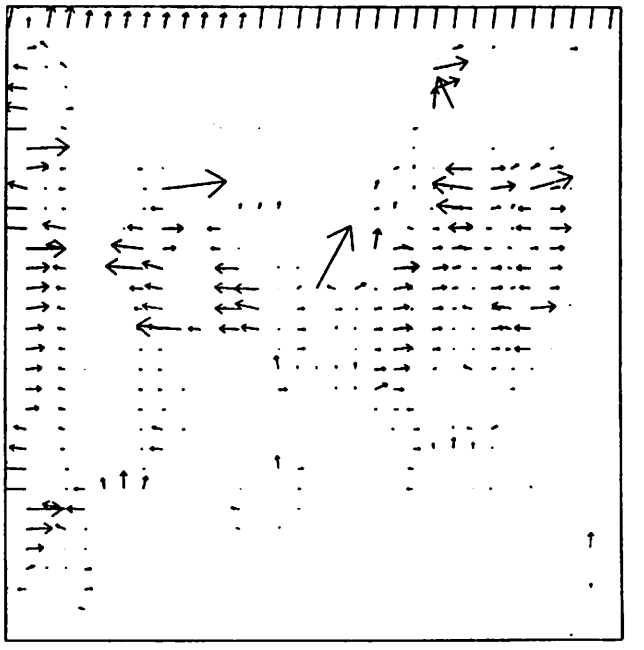

Fig. 8: Experiment 2: a 32×32 sample of the maximal component of the directional confidence measure. Notice the high confidence assigned to the normal component of displacements near straight lines.

$[1., 100.)$, using the transformation $W' = (100W + 1)/(W + 1)$. Then, a scalar confidence measure was derived from the directional confidence measure using the relation (25). A selection of 256 vectors from the displacement field was performed, based on two criteria: high values of the scalar confidence measure, and a uniform distribution over the image.

The 3-D motion parameters were computed from the selected vectors by minimizing either Eq. (11), using the scalar confidence measure, or Eq. (15), using the directional confidence measure. In the first case we estimated the value of $\underline{U}$ as $(0.005, -0.020, 1.000)$, which is a deviation of $1.15°$ from the line of sight, and the value of $\underline{\Omega}$ as $(-0.035°, -0.112°, -0.652°)$. The results in the second case were almost identical.

In the last stage, the relative depth values were computed using either Eq. (10) or Eq. (14). In both cases (see Figs. 9 and 10) the depth values usually vary smoothly, unfortunately even across occlusion boundaries, due to the smoothness process in Anandan's technique. The results obtained by using the directional confidence measure seem to be somewhat better in this sense. The overall improvement is not significant however, because the tangential components of displacement vectors at edge points are almost as accurate as the normal components. This was achieved by employing the directional confidence measure as a tool in the smoothness process. To conclude, the directional confidence measure did not significantly improve the 3-D interpretation, since it did not reflect the accuracy of the displacement measurements.

7.3 Experiment 3 The input to this experiment is a list of line segment pairs, where the lines were extracted by the method described in [Bol87], and matched by the algorithm presented in [Wil88]. This experiment demonstrates the ability to recover 3-D motion and structure from line segments, using only two frames. As in the previous experiment, the

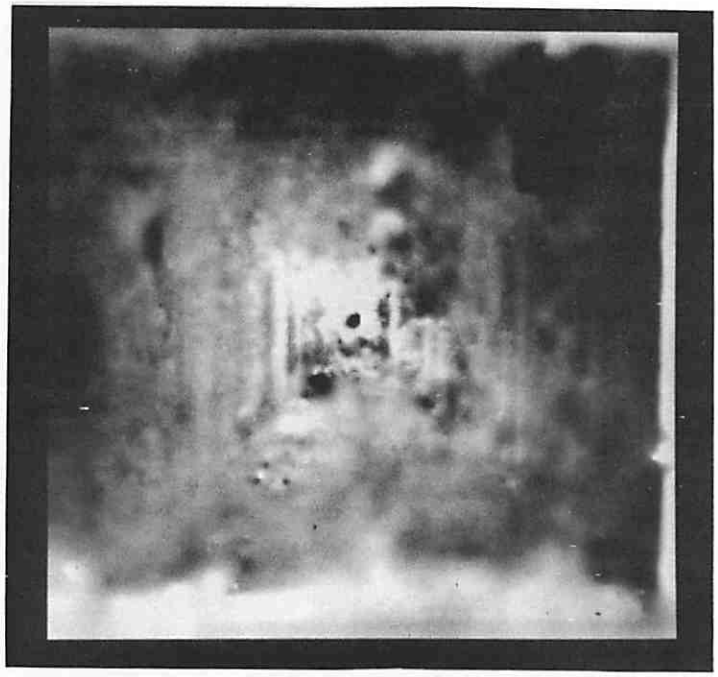

Fig. 9: Experiment 2: The depth map obtained by using the scalar confidence measure. The depth values are encoded by intensity (more distant surfaces are brighter).

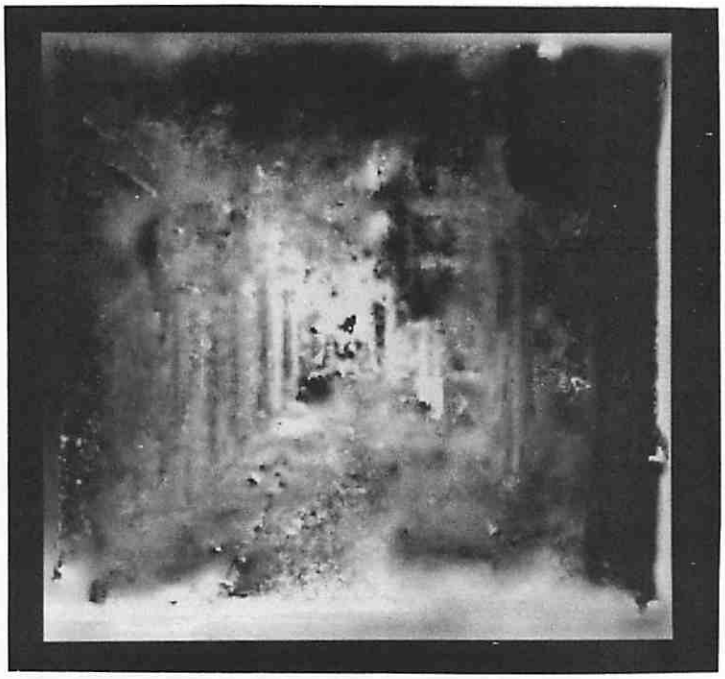

Fig. 10: Experiment 2: The depth map obtained by using the directional confidence measure.

intensity images contain 256×256 pixels and correspond to field of view of $25°$. The first image is shown in Fig. 11, and the line segments computed for this image are shown in Fig. 12. The estimation of 3-D information was based on endpoint correspondences obtained from the list of line matches.

The endpoint pairs were grouped into two sets according to their reliability. This grouping affects the determination of the confidence measure, as explained in the following paragraph. In the set of unreliable correspondences, we included pairs associated with non-unique line matches or with matches where one segment was more then 20% longer than the other segment. We also included in this set pairs where one of the endpoints was less than 2.5 pixels away from the image boundary. All the other endpoint pairs were included in the set of reliable correspondences.

A directional confidence measure was determined for the displacement vector obtained from each endpoint pair. The direction of minimal confidence was estimated as the average orientation of the lines associated with the pair. For the reliable pairs, the standard deviations, σ_t and σ_l, of the transverse and longitudinal measurement errors, were estimated as 0.25 and 1 (in pixels), respectively. Hence, the corresponding confidence values were selected to be $W_t = 16$ and $W_l = 1$. For the unreliable pairs, we still selected $W_t = 16$, but W_l was determined to be 0. Thus, these pairs did not participate in the computation of the 3-D motion parameters, but their depth was estimated.

The 3-D motion and structure were computed using either a scalar confidence measure, or a directional confidence measure. In the first case, the same scalar weight was assigned to each of the more reliable endpoint pairs. The motion parameters found in this case were $\underline{U} = (0.045, 0.058, 0.997)$, corresponding to a deviation of $4.23°$ from the line of sight, and

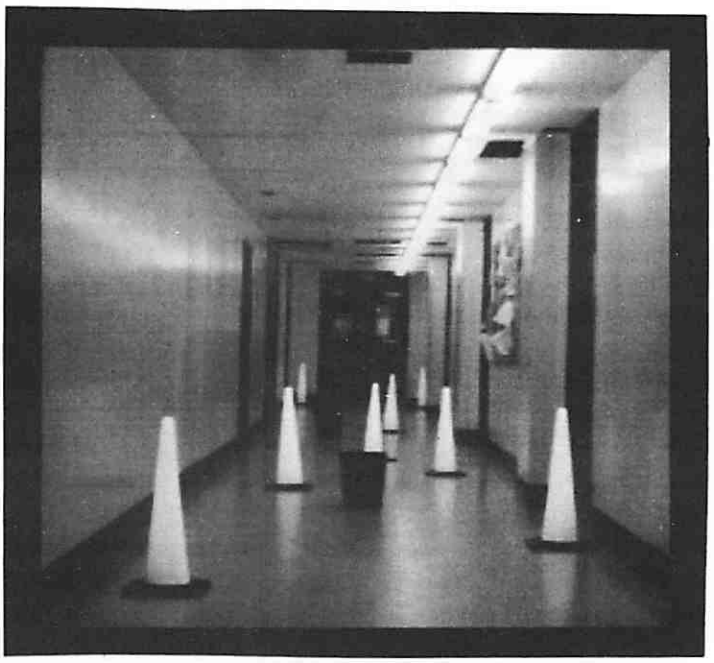

Fig. 11: Experiment 3: The first intensity image.

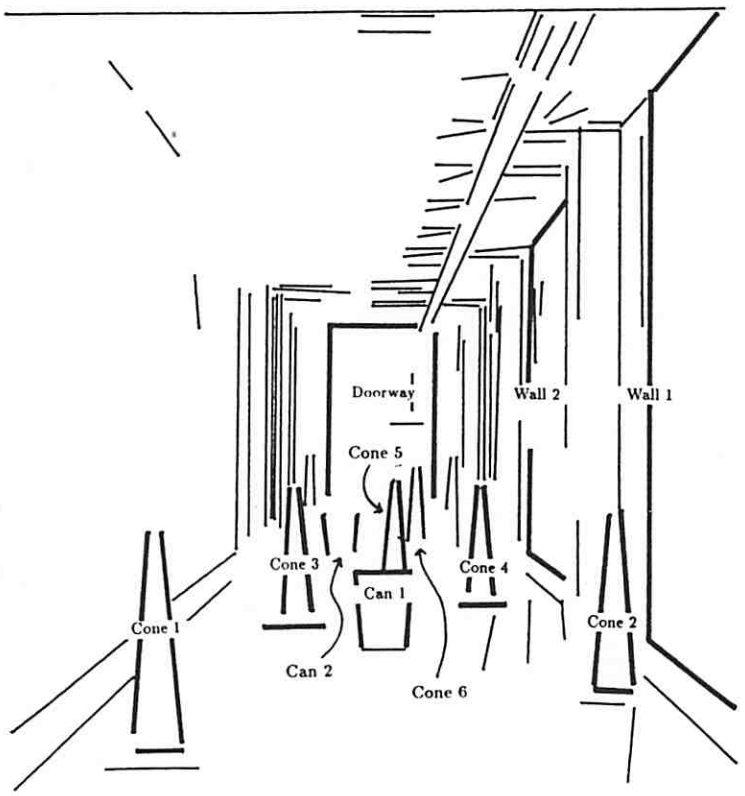

Fig. 12: Experiment 3: The line segments extracted from the first image. Objects with known depth values are labeled.

$\underline{\Omega} = (0.250°, 0.096°, -0.033°)$. In the second case, using a directional confidence measure, the vector $\underline{U}$ was found to be $(0.008, -0.011, 1.000)$, deviating $0.77°$ from the line of sight, and the rotation vector $\underline{\Omega}$ was estimated as $(0.087°, 0.204°, 0.041°)$.

In this experiment, the actual depth values of some of the objects in the scene are known. In addition, the translation magnitude is known to be 1.95 feet. In Table 2, we compare the estimated depth values computed by each of the algorithms to the ground truth values. For most objects, the estimates obtained by employing the directional confidence measure are significantly better than the estimates corresponding to the scalar confidence measure. The results for Cone 5 and Cone 6 are exceptional, because the related lines are oriented towards the FOE, and their longitudinal displacements are almost as accurate as the transverse displacements.

Object	Ground Truth	#Pairs	Scalar Conf. – Average Error	Direct. Conf. – Average Error	Direct. Conf. – Aver. Norm. Err.
Cone 1	20.0 ft	8	11.5%	2.2%	0.88
Cone 2	25.0 ft	8	56.5%	1.8%	0.48
Wall 1	27.1 ft	4	7.1 %	5.6%	1.02
Can 1	30.0 ft	6	13.0%	6.8%	0.42
Cone 3	35.0 ft	6	14.6%	5.2%	0.45
Cone 4	40.0 ft	6	7.9%	6.2%	0.49
Cone 5	45.0 ft	4	13.0%	81.9%	1.01
Wall 2	48.7 ft	6	57.2%	39.8%	0.64
Can 2	55.0 ft	2	51.1%	55.5%	0.49
Cone 6	60.0 ft	4	32.8%	67.9%	1.09
Doorway	87.1 ft	8	91.3%	57.4%	0.84

Table 2: Experiment 3. For each object the following data is shown: the ground truth value, the number of endpoint pairs, the average value of errors $|\Delta\tilde{Z}|/\tilde{Z}$, both for the scalar confidence measure and for the directional confidence measure, and the average value of $|\Delta\tilde{Z}|/\sigma(\tilde{Z})$ for the directional measure.

The depth errors associated with the directional confidence measure were normalized to units of their estimated standard deviations. In other words, the ratios $|\Delta\tilde{Z}|/\sigma(\tilde{Z})$ were computed, using Eq. (27) for estimating $\sigma(\tilde{Z})$. For each object, the average of these normalized errors was computed (see Table 2). These average values vary between 0.42 and 1.09, thus, demonstrating the predictability of the actual depth errors from their estimated standard deviations. This shows that Eq. (27) can be used successfully to distinguish between reliable and unreliable estimates.

8. SUMMARY

The directional confidence measure is a numerical representation of the expected reliability of image flow estimates. A scheme for incorporating this measure into a least squares technique for computing 3-D motion and structure from a flow field was introduced. A confidence measure for the depth estimates was also presented, and relations between these measures and between expected errors of the flow estimates were established.

The ability to employ a directional confidence measure was found to be especially useful in the case of line segment correspondences. Experimental results demonstrated the superiority of this measure over a scalar confidence measure in cases where the reliability of the image flow is orientation dependent and can reasonably be estimated.

ACKNOWLEDGEMENTS

We would like to thank many members of the computer vision group at UMass for useful discussions. Special thanks are also due to Lance Williams, Harpreet Sawhney and P. Anandan for providing the data for Experiments 2 and 3.

REFERENCES

[Adi85a] G. Adiv, "Determining 3-D Motion and Structure from Optical Flow Generated by Several Moving Objects", *IEEE Trans. Pattern Anal. Machine Intell.*, vol. PAMI-7, pp. 384–401, July 1985.

[Adi85b] G. Adiv, "Interpreting Optical Flow", Ph.D Dissertation, Computer and Information Science Dept., Univ. of Mass., 1985.

[Adi89] G. Adiv, "Inherent Ambiguities in Recovering 3-D Motion and Structure from a Noisy Flow Field", to appear in *IEEE Trans. Pattern Anal. Machine Intell.*, 1989.

[Ana84] P. Anandan, "Computing Dense Displacement Fields with Confidence Measures in Scenes Containing Occlusion", in *Proc. DARPA Image Understanding Workshop*, New Orleans, Louisiana, 1984, pp. 236–246.

[Ana87] P. Anandan, "Measuring Visual Motion from Image Sequences", Ph.D. Dissertation, Computer and Information Science Dept., Univ. of Mass., 1987.

[Ana88] P. Anandan, "A Computational Framework and an Algorithm for the Measurement of Visual Motion", to appear in *International Journal of Computer Vision*, 1988.

[Bol87] M. Boldt and R. Weiss, "Token-Based Extraction of Straight Lines", TR 87-104, Computer and Information Science Dept., Univ. of Mass., Amherst, Mass., October 1987.

[Bru81] A.R. Bruss and B.K.P. Horn, "Passive Navigation", MIT A.I. Memo 662, 1981.

[Dut88] R. Dutta, R. Manmatha, E.M. Riseman and M.A. Snyder, "Issues in Extracting Motion Parameters and Depth from Approximate Translational Motion", in *Proc. DARPA Image Understanding Workshop*, Cambridge, MA, 1988, pp. 945–960.

[Fau87] O.D. Faugeras, F. Lustman and G. Toscani, "Motion and Structure from Motion from Point and Line Matches", in *Proc. 1st Int. Conf. Computer Vision*, London, 1987, pp. 25–34.

[Liu88] Y. Liu and T.S. Huang, "Estimation of Rigid Body Motion Using Line Correspondences", *Computer Vision, Graphics and Image Processing*, vol. 43, pp. 37–52, 1988.

[Lon81] H.C. Longuet-Higgins, "A Computer Algorithm for Reconstructing a Scene from Two Projections", *Nature*, vol. 293, pp. 133–135, Sep. 1981.

[Med85] G. Medioni and Y. Yasumoto, "Robust Estimation of 3-D Motion Parameters

from a Sequence of Image Frames Using Regularization", in *Proc. DARPA Image Understanding Workshop*, Miami Beach, Florida, 1985, pp. 117–128.

[Nag86] H. H. Nagel and W. Enkelman, "An Investigation of Smoothness Constraints for the Estimation of Displacement Vector Fields from Image Sequences", *IEEE Trans. Pattern Anal. Machine Intell.* Vol. PAMI-8, pp. 565-593, 1986.

[Spe87] M.E. Spetsakis and J. Aloimonos, "Closed Form Solution to the Structure from Motion Problem from Line Correspondences", in *Proc. Sixth National Conf. Artif. Intell.*, Seattle, WA, 1987, pp. 738–743.

[Tsa84] R.Y. Tsai and T.S. Huang, "Uniqueness and Estimation of Three-Dimensional Motion Parameters of Rigid Objects with Curved Surfaces", *IEEE Trans. Pattern Anal. Machine Intell.*, vol. PAMI-6, pp. 13–27, Jan. 1984.

[Ull79] S. Ullman, "The Interpretation of Visual Motion". Cambridge, MA: MIT Press, 1979.

[Wel87] W.M. Wells III, "Visual Estimation of 3-D Line Segments From Motion — A Mobile Robot Vision System", in *Proc. Sixth National Conf. Artif. Intell.*, Seattle, WA, 1987, pp. 772–776.

[Wil88] L.R. Williams and A.R. Hanson, "Translating Optical Flow into Token Matches", in *Proc. of DARPA Image Understanding Workshop*, Cambridge, Mass., 1988, pp. 970–980.